Flexion, Extension and Lateral Bending Responses of the Cervical Spine

James H. McElhaney, Brian J. Doherty, Jacqueline G. Paver,
Barry S. Myers and Linda Grey*

Biomedical Engineering Department
*Department of Radiology
Duke University, Durham, N.C. 27706

ABSTRACT

The lateral, anterior and posterior passive bending responses of the human cervical spine were investigated using unembalmed cervical spinal elements obtained from cadavers. Bending stiffness was measured in six modes ranging from tension~extension through compression~flexion. A five-axis load cell was used to establish the end conditions. Results include moment-angle curves, relaxation moduli and the effect of cyclic conditioning on bending stiffness. The Hybrid III ATD neck was also tested and its responses are compared with the human. It was observed that the Hybrid III neck was more rate sensitive than the human, that mechanical conditioning significantly changed the stiffness of the human specimens and that changing the end condition from pinned-pinned to fixed-pinned increased the stiffness by a large factor. The bending stiffness was significantly influenced by the direction of the bending moment, the type of end restraint, the magnitude of the deformation and the previous deformation history. The shear force produced by the end conditions was an important factor in the applied moment. This shear force not only changes the moment acting on the specimen but also influences the failure mode. These experiments indicate that when the loading is eccentric (as it almost always is), the primary deformation mode is bending, and the moment applied to the specimen is strongly influenced by shear forces and the magnitude of the eccentricity. The axial load is therefore a poor indicator of the type and magnitude of failure stresses.

MR and CT was used to visualize the damage after loading. When compared to the dissection results MR was clearly superior to CT in detecting soft tissue and ligamentous injuries.

INTRODUCTION

The majority of the studies of the structural properties of the spine have involved compression. Perhaps the earliest such study was Messerer's work on the mechanical properties of the vertebrae (2). He reported compression breaking loads ranging from 1.47-2.16 kN for the lower cervical spine. Bauze and Ardran loaded human cadaveric cervical spines in compression and reported forward dislocations with loads of 1.32-1.42 kN (3). However, their experiments were designed to force the dislocations to occur at a given vertebral level. Sances tested isolated cadaver cervical spines in compression, tension and shear (4). A quasi-static compression failure was observed at a load of 0.645 kN, and dynamic compression-flexion failures were reported at loads ranging from 1.78-4.45 kN. McElhaney *et al.* applied time-varying compressive loading to unembalmed human cervical spines (5,6). Failures were produced which are similar to those observed clinically with maximum loads ranging from 1.93-6.84 kN. In addition, it was found that small eccentricities in the load axis could change the buckling mode from posterior to anterior. Panjabi *et al.* measured rotation and translation of the upper vertebra as a function of transection of the components in single units of the cervical spine (7). Selecki and Williams conducted a study of cadaveric cervical spines loaded with a manually operated hydraulic jack (8). They were able to duplicate several types of clinically observed injuries, but reported loads in terms of the hydraulic pressure. Nusholtz *et al.* studied neck motions and failure mechanisms on unembalmed cadavers due to crown impacts; failure loads ranged from 3.2 to 10.8 kN (9). They reported that spinal response and damage were significantly influenced by the initial configuration of the spine.

Very few tests have been conducted on longer spinal segments. Edwards *et al.* tested lumbar spine motion units in combined loading (10). They found that stiffness of the motion unit was nonlinear and increased with increasing load. Markolf and Steidel tested human cadaveric thoracolumbar spine motion units in flexion, extension, lateral bending, torsion, and tension (11). They conducted free-vibration tests, and reported stiffness and damping values for the various test modes and vertebral levels. Panjabi *et al.* measured the three-dimensional stiffness matrix for all levels of the thoracic spine by measuring all components of deflection of spinal units for various loading modes (12). Roaf loaded single cervical spinal units in compression, extension, flexion, horizontal shear, and rotation (torsion) (13). He found that the intact disc, which failed at approximately 7.14 kN, was more resistant to compression than wet vertebrae which failed at approximately 6.23 kN. It is his contention that ligamentous rupture cannot be caused by hyperflexion or hyperextension, but only by rotation and/or shear forces. Tencer *et al.* performed static tests on individual lumbar spinal units (14). They presented load-deflection data for all loading modes. Hodgson measured the strain at selected locations of the cervical vertebrae of cadavers under several head impact modes (15). He concluded that the effects of off-axis, torsional and transverse shear are important variables and influence the axial response. Seemann compared the dynamic responses of the human and Hybrid III neck (16). He concluded that there was a good match with some bending modes but a poor one in others. An extensive review of the literature was presented by Sances 1981 (1).

A major problem with tests on spinal elements has been the proper measurement of the forces and moments applied to the specimen. The experiments reported here used a five-axis load cell in an attempt to better understand the reasons for the wide range of compressive failure loads and failure mechanisms reported in the literature.

METHODS

SPECIMEN TYPES AND PROCUREMENT – Unembalmed human cervical spines were obtained shortly after death, sprayed with calcium buffered, isotonic saline, sealed in plastic bags, frozen and stored at -20°C. Cervical spine specimens generally included the base of the skull, approximately two centimeters around the foramen, or C1 at the superior end and C5, C6, C7, or T1 at the inferior end. The associated ligamentous structures were kept intact. X-rays were taken and reviewed to assess specimen integrity. Medical records of donors were examined to ensure that the specimens were normal for their age group and did not show evidence of serious degeneration, spinal disease, or other health-related problems that would affect their structural responses.

SPECIMEN PREPARATION – Prior to testing, each specimen was thawed at 20°C for 12 hours. The pre-test specimen preparation was performed in an environmental chamber, which was designed to prevent specimen dehydration and deterioration. A variable flow humidifier pumped water vapor into the chamber to create a 100% humidity environment. The end vertebrae were cleaned, dried, and defatted for casting. The specimen was mounted in aluminum cups with a pin inserted into the spinal canal in order to provide a reference bending axis. Using polyester resin, the ends of the specimens were cast in the cups so that the cups were approximately perpendicular to the axes of the end vertebrae (17). During casting, the aluminum cups were cooled in a flowing water bath to minimize degradation due to the heat of polymerization.

TEST INSTRUMENTATION – A Minneapolis Test Systems (MTS) servo-controlled hydraulic testing machine was used to conduct the various viscoelastic tests. The first series was axial compression using a spherical washer to minimize the moments at the ends. A lead screw adjustment at the lower end was used to straighten the lordotic curve and align the specimen (Figure 1).

The second series was a combination of bending and axial loading. An eight-channel transducing system was used to measure the axial, lateral, and anterior forces, the flexion-extension and lateral bending moments, the linear motion of the ram, and the angular motion of the specimen ends. Loads and moments were measured with a five-axis load cell assembly, which was constructed using two GSE three-axis ATD neck load cells. The motion of the specimen ends was measured with an internal coaxial linear variable differential transformer (LVDT) and two external rotational variable differential transformers (RVDT). These transducers provided data to establish the motion of the two specimen ends from direct measurements of the total bending angle and calculations of the specimen length change. The internal LVDT was used to monitor the ram motion and hence the displacement of the clevis end of the lower transfer bar. One external RVDT was used in the pinned-pinned and fixed-pinned tests to track the rotation of the specimen end of the lower transfer bar relative to the ram; the second external RVDT was used in the pinned-pinned tests to track the rotation of the specimen end of the upper transfer bar. Figure 2 is a schematic diagram of the test apparatus.

A digital measurement and analysis system was developed utilizing a data logging computer. The multichannel microcomputer-based data acquisition system incorporated an RC Electronics ISC-16 Computerscope for the digitization and storage of data. This system, which consists of a 16-channel A/D board, external instrument interface box, and

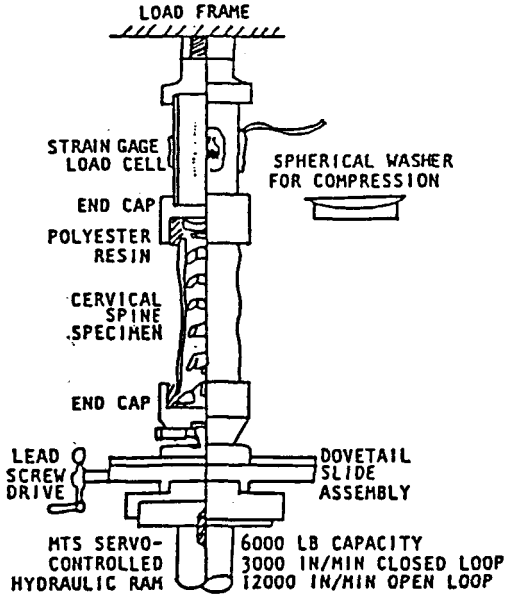

Figure 1. Axial Compression Test Fixture.

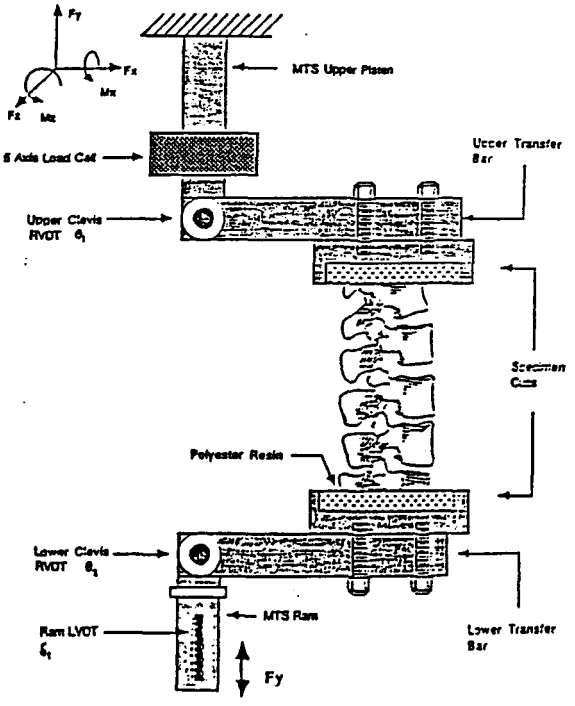

Figure 2. Free-Free Test Configuration

Scope Driver software, has a 1 MHz aggregate sampling rate capability with 12 bit resolution and writes data directly to a hard disk. In addition, during the failure tests, flouroscopic images were recorded on videotape.

THE COMBINED AXIAL LOADING – BENDING TEST APPARATUS – A specially designed test jig was developed to place the specimen in a state of eccentric axial loading. This resulted in a combined axial load and bending moment applied at the ends of the specimen. The apparatus provided adjustable moment arms and accommodated the following six test modes: compression-flexion (CF), tension-flexion (TF), compression-extension (CE), tension-extension (TE), compression-lateral bending (CL), and tension-lateral bending (TL). Two test configurations were utilized: (1) pinned-pinned end conditions (PP), and (2) fixed-pinned end conditions (FP).

For the pinned-pinned end conditions, the upper transfer bar was attached via a clevis to the load cell assembly, which was rigidly mounted to the upper platen of the MTS. The lower transfer bar was attached via a clevis to the ram of the MTS. The centerline of the specimen was parallel to, but not coincident with, the line of action of the MTS ram. The clevis end of the upper transfer bar was constrained from translation. The two external RVDTs were mounted on the test apparatus in order to measure the angular displacement of each transfer arm. In this configuration, the specimen was mounted with the superior end attached to the upper transfer bar and the inferior end attached to the lower transfer bar.

For the fixed-pinned end conditions, the upper clevis and corresponding RVDT were removed. In this configuration, the specimen was mounted with the superior end attached to the pivoting lower transfer bar and the inferior end fixed to the load cell assembly, which was rigidly mounted to the upper platen of the MTS.

A free body diagram of the test configuration is presented in Figure 3. The reference center line of the specimen is the central axis of the spinal foramen. The moment at the center of the specimen is

$$M_A = P_y a - P_x b,$$

and the moment measured by the load cell is

$$M_O = P_x B.$$

The moment induced by the shear force P_x was significant in the fixed-pinned configuration but was negligible in the pinned-pinned configuration. The apparatus had minimal overshoot and vibration below test frequencies of 5 Hz. Inertial forces begin to predominate above 10 Hz, and this is the current system's upper frequency range.

In this paper, test rates will be described in Hertz. The test period is the reciprocal of the frequency, and the time to peak load is one-half of the test period. The deformation rate is the maximum deformation in angular or linear units multiplied by twice the test frequency.

CONSTANT VELOCITY TESTS – Constant velocity tests were conducted on mechanically stabilized spines using triangle wave deformations at frequencies of 0.01, 0.1, 1.0, 5 Hz, and, for some specimens, 10 Hz. Thus, the deformation rate was varied by a factor of 500-1000.

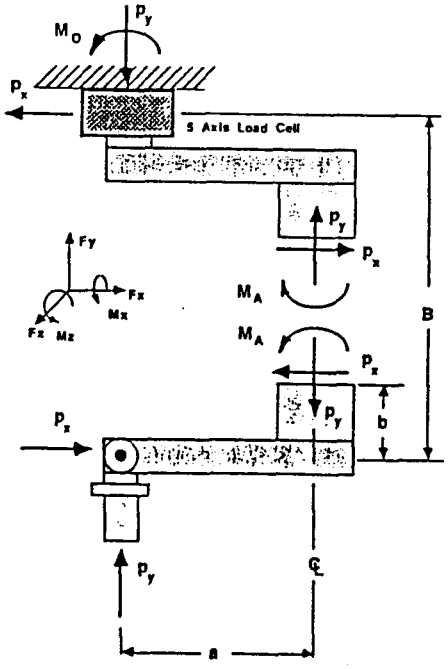

Figure 3. Freebody Diagram for the Fixed-Pinned Test Configuration.

TABLE 1. CONSTANT VELOCITY STIFFNESS (N-m/rad).

MODES	HUMAN						HYBRID III	
	FIXED-PINNED			PINNED-PINNED			FIXED-PINNED	PINNED-PINNED
	Mean	σ	N	Mean	σ	N	Mean	Mean
CF	29.9	2.6	10	8.1	0.7	5	589.1	150.8
TF	41.8	5.6	5	14.8	1.3	5	608.4	199.0
CE				2.8	0.6	9	795.7	122.5
TE	309.0	26.9	5	10.3	1.2	11	232.1	138.8
CL	8.7	0.6	10	3.1	1.0	17	898.9	190.9
TL	254.1	34.6	5	13.0	1.9	5	442.0	226.1

σ = Standard Deviation; N = Number of Tests.

Table 1 shows the stiffness averaged over four rates for all specimens. Three distinct tests of the Hybrid III were performed so that each value represents the mean of 12 tests. Several observations are apparent from this data. First, there are significant differences between the bending stiffnesses of the cadaver cervical spine and the Hybrid III. Second, there are significant differences in the bending stiffness of the cadaver cervical spine in the different modes. Tension-extension was the largest with a stiffness of 125 N-m/Radian, fixed-pinned and 15 N-m/Radian, pinned-pinned. Compression-lateral was the smallest with a stiffness of 10 N-m/Radian, fixed-pinned and 2.6 N-m/Radian pinned-pinned.

Figure 6 shows a typical response pattern for the human cervical spine to the various combined bending and axial loading modes. Figure 7 shows a typical response pattern for the Hybrid III.

Constant velocity testing in axial compression was also performed on fourteen specimens. The average stiffness per motion segment was 571 newtons per centimeter. Typical test results for a single motion segment are shown in Figure 8.

FAILURE TESTS – After the battery of viscoelastic tests was accomplished, a constant velocity failure test at 0.1 Hz was performed on the bending test specimens. This rate was used so that flouroscopic images of the specimen motion could be obtained. All failure tests were in the compression-flexion mode (CF). After the tests the specimens were examined with magnetic resonance imaging (MRI) and computerized tomographic radiography (CT), then dissected. Table 2 provides the maximum moment axial force and shear force applied to the specimen and the bending angle at which these peaks occurred. The first four tests (1C, 2C, 3C, 4C) were performed in the pinned-pinned mode and the remainder (6C, 7C) were tested in the fixed-pinned mode. In the pinned-pinned configuration the specimens were very flexible and were able to bend through on average of 45 degrees without an unstable dislocation. These specimens contained C_1 through T_1 and seven intact intervertebral structures. This is approximately 6.4 degrees per vertebral level. The shear forces were very small. The axial forces were low enough that the major stresses were due to the bending moment. The primary failure mechanism was disruption of the interspinous ligaments (ligamentum nuchae), the ligamentum flavum and capsular ligaments. There was also minor anterior wedging of the middle vertebral bodies and discs. In the pinned-pinned configuration the moment is maximum in the middle of the specimen. This may be the reason that the most frequent spinal cord injury level observed clinically is C_4 - C_5 and C_5 - C_6 (5).

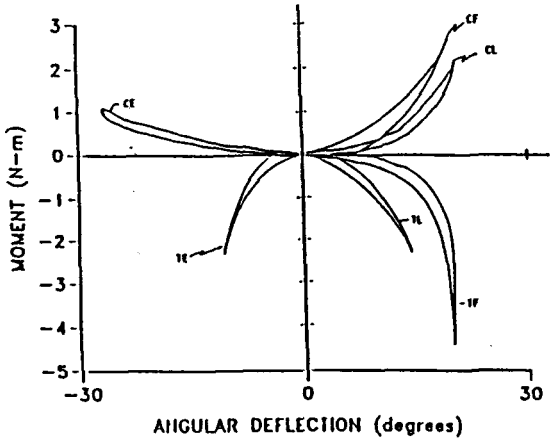

Figure 6. Typical Bending Responses of Human Cervical Spine.

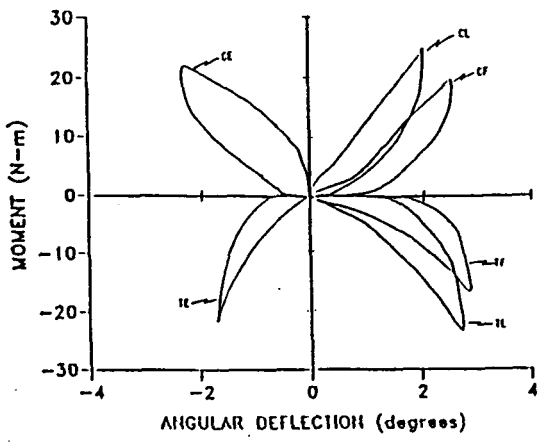

Figure 7. Typical Bending Responses of Hybrid III Neckform.

Typical constant velocity moment-angle curves are presented for human and Hybrid III cervical spines in the pinned-pinned and fixed-pinned test configuration in Figures 4 and 5. All of the curves exhibit a hardening response (increasing stiffness) and hysteresis. The human and Hybrid III responses are fundamentally different. The Hybrid III shows the classic linear viscoelastic response of increasing stiffness with displacement rate while the human shows little change in stiffness or hysteresis over the rate range tested. Since these features of hysteresis, relaxation, and stiffness are not very sensitive to the rate of strain, simple linear viscoelastic models would not be appropriate predictors of the time dependent human spinal bending responses; and the more complex Maxwell-Weichert quasi-linear model is required (6).

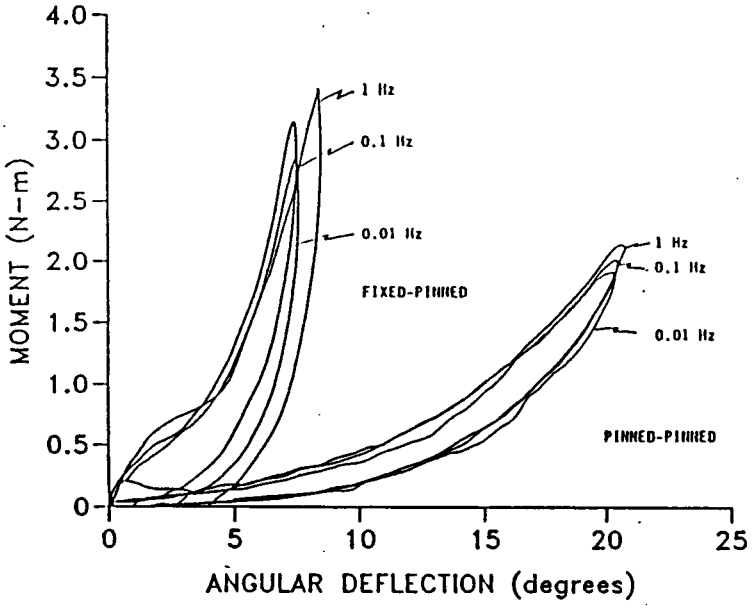

Figure 4. Typical Constant Velocity Profile for Human Cervical Spine (Compression-Flexion).

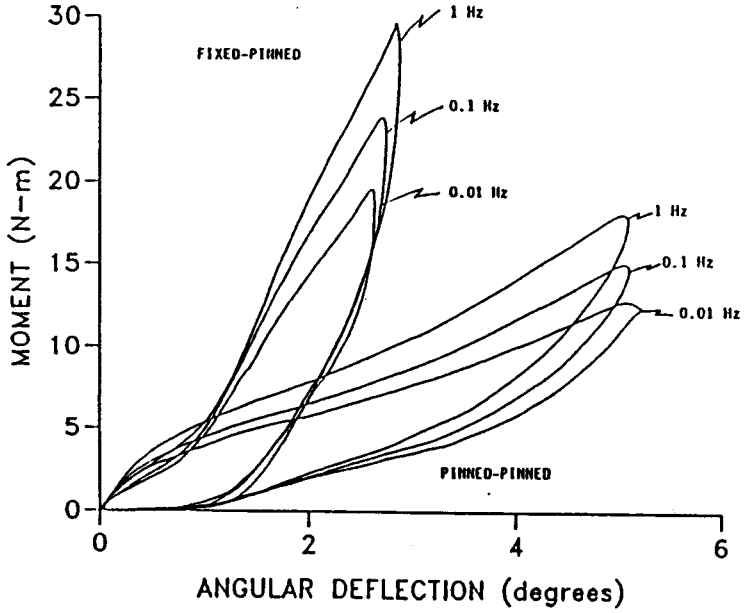

Figure 5. Typical Constant Velocity Profile for Hybrid III Neckform (Compression-Flexion).

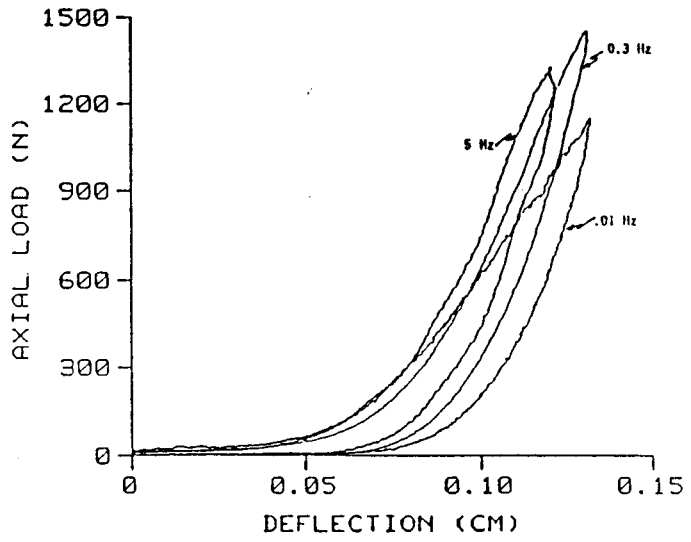

Figure 8. Typical Constant Velocity Axial Load Response C5-C6 Motion Segment.

TABLE 2. FAILURE TEST RESULTS.

SPECIMEN NUMBER	AGE/ SEX	VERTEBRAL LEVELS	MAXIMUM MOMENT (N-m)	MAXIMUM AXIAL FORCE (N)	MAXIMUM A-P SHEAR (N)	ANGLE AT MAX.MOMENT (deg)	FAILURE CLASSIFICATION
1C P-P	52/M	$C_1 - T_1$	14.6	192	0	54	C_4-C_5, C_5-C_6 ligamentum nuchae, ligamentum flavum, and post. long. ligament torn
2C P-P	64/F	$C_1 - T_1$	8.75	214	0	57	C_6-C_7 ligamentum nuchae and R capsular ligament torn
3C P-P	N/A	$C_1 - T_1$	3.01	108	0	31	wedging of C_4-C_5 bodies, C_5-C_6 ligamentum nuchae disrupted
4C P-P	69/M	$C_1 - T_1$	3.40	338	11.7	40	wedging and broadening of C_4-C_5 and C_5-C_6 bodies, tear of C_3-C_4 disc
5C P-F	77/M	$C_1 - T_1$					this specimen was not loaded to failure
6C P-F	76/M	$BOS - T_1$	6.7	1513	23.0	15	C_4-C_5 ant. disc disrupted, C_2-C_3, C_3-C_4, C_4-C_5 L capsular ligaments partially disrupted
7C P-F	86/M	$BOS - T_1$	10.2	2305	35	22	C_4-C_5, C_5-C_6, C_6-C_7 shortened discs and wedged bodies, disrupted C_7-T_1 disc, ligamentum nuchae and ligamentum flavum stretched

In the fixed-pinned configuration much larger axial forces are required to produce the same bending moment because the shear force produces a counteracting moment. This is reflected in the failure mechanisms by superimposing compressively induced failures (wedging of bodies and discs) to the posterior tensile failures due to bending.

Figure 9 shows a composite of the moment-angle diagrams for the failure tests. The maximum moment ranged from 3.01 to 14.6 N-m. This large range is probably due to the variation in the size of the specimens. Specimen 1C and 7C had much larger vertebrae than the others as demonstrated by the CT scans.

In the axial compression mode the failure test was performed at a ram velocity of 64 cm/sec.

Table 3 summarizes the type of failure, the maximum load and deflections, and the strain energy or area under the loading portion of the load~deflection curve failure. Figure 10 shows a representative curve.

The following four failure mechanisms were observed for the axial compression tests.

EXTENSION/COMPRESSION – As the body, discs and facet joints resisted the load, the posterior elements were compressed and, as failure of the disc and end plates occurred, the cervical spine extended in a forward buckling mode. Specimen A80-339 failed in this way with rupture of the anterior longitudinal ligament and distraction of the anterior section of the disc between C4 and C5. This occurred with a one centimeter posterior eccentricity.

JEFFERSON FRACTURES – In the clinical literature, the common etiology of a fracture of the atlas is a direct blow to the top of the head. In these tests, the experimentally produced atlas fractures, which were usually bilateral and symmetrical, involved the anterior and posterior arches. This was probably due to the compressive force driving the articular condyles outward and bending the arches.

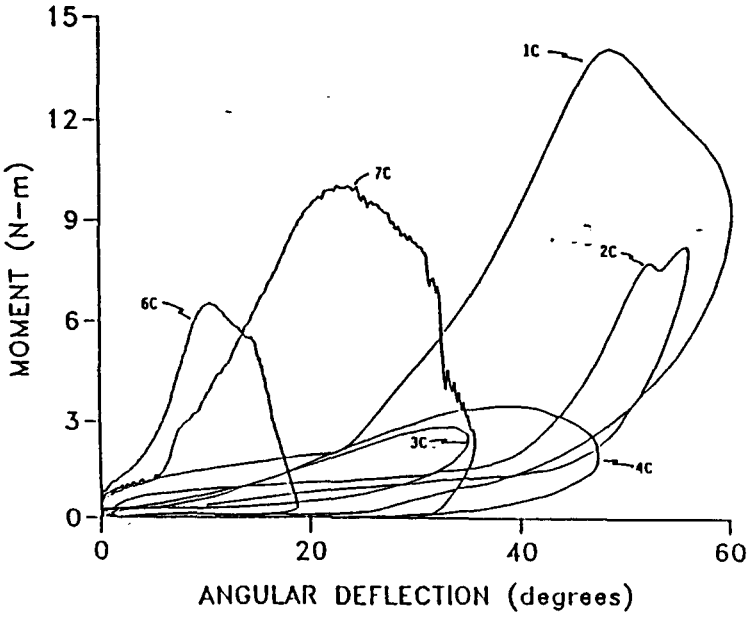

Figure 9. Failure Curves -- Compression-Flexion.

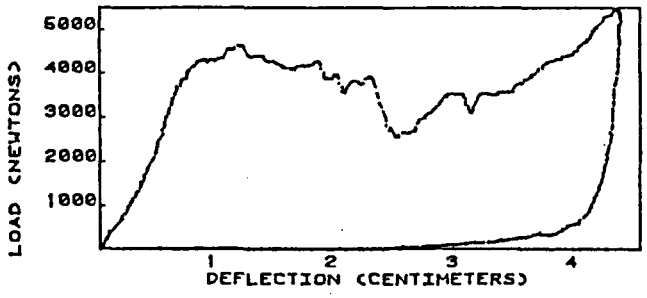

Figure 10. Typical Axial Compression Test (A83-26).

TABLE 3. AXIAL COMPRESSION FAILURE TESTS.

Specimen Number	Age (years) Sex	Description	Failure Mode	C5 Area (cm^2)	Max. Load (N)	Max. Deflection (cm)	Strain Energy (N-cm)
A79-409	58M	B.O.S.* to T2	Jefferson Fr.	5.71	3560	3.0	7470
A79-415	37M	B.O.S. to T1	Compression C5	5.98	5340	3.0	12800
A79-419	49F	B.O.S. to T2	Compression C4&C5	4.29	4860	3.0	10300
A79-423	52M	B.O.S. to T1	Jefferson Fr.	6.17	4190	3.0	7920
A79-431	46M	B.O.S. to T1	Anterior Wedge C5	6.30	4720	3.0	9340
A80-289	70M	B.O.S. to C7	C2 Cracked	5.43	5010	2.9	7950
Retest		C3 to C7	Anterior Wedge C6		6040	2.7	10900
A80-339	62F	B.O.S. to T1	Extension Failure	3.51	1930	4.0	4480
A80-352	62M	B.O.S. to C6	Jefferson Fr.	6.58	3120	3.0	5740
A80-357	46F	B.O.S. to C6	Jefferson Fr.	3.71	960	2.9	1800
A80-364	41M	B.O.S. to C6	C1&C2 Fractured	5.62	5270	2.5	8550
A80-368	77M	B.O.S. to C6 C3,4,5 Bodies Fused	C1 Fractured	5.77	3650	2.7	6350
A80-384	64F	B.O.S. to C7	C2 Fractured	4.38	4060	4.5	12300
Retest		C3 to C7	Burst C4 and Anterior Wedge C4&C5		6840	3.5	15500
A83-26	44M	C2 to T2	Burst Fracture C3, C4&C5	5.45	5470	4.4	15600
A83-42	63F	B.O.S. to C6	Burst Fracture C3&C6	3.28	3000	2.8	5550

*B.O.S. = Base of Skull

BURST FRACTURES – Comminuted vertical fractures through the vertebral body produced framentation of the centrum into a number of large pieces. There were no obvious areas of compressed cancellous bone. Analysis of x-rays taken before and after each test indicated that the specimens that burst were slightly flexed to straight while the specimens that sustained the Jefferson fractures were slightly extended to straight. The burst fractures required larger forces and strain energies than the Jefferson fractures. The load~deflection diagram exhibited a characteristic M-shape or twin peak. Specimen A80-384 showed multiple spikes in the first peak which may be related to the multiple fracturing process.

ANTERIOR WEDGING – The addition of the small flexing moment arm ($h < 1$ cm) using the test fixture resulted in compression and fracture of the anterior section of the vertebral body. The addition of a slightly larger moment arm ($h = 1$ cm) produced buckling rearward. Pieces of the cortical shell were displaced in a random pattern. End plate failure occurred and the intervertebral disc was disrupted. However, the amount of displacement applied to the specimen did not result in large anterior dislocation or rupture of the anterior longitudinal ligament. By careful alignment and adjustment of the slide-positioning device, we were able to produce fractures similar to those observed clinically. But, after fourteen tests, we had the distinct impression that one or two centimeters forward or backward, right or left, made a tremendous difference in the outcome. Perhaps, this is the reason there is such a wide range of responses to cervical spine compression in the relevant literature.

SUMMARY – In the engineering disciplines, a designer starts with a basic building material and shapes it into a structure with specified load and deformation responses. These load and deformation responses are defined as the structural properties. The structural properties are determined by the size, shape, configuration and material of which a structure is composed. In contrast, the material properties are independent of the structure or shape of the material under consideration. Since the human body exists, it exhibits load and deformation responses which determine its injury potential in traumatic environments. Knowledge of the properties of the material of which the human body is composed is useful in so far as it leads to a better understanding of these structural properties.

This study demonstrated the complex, time-dependent responses of the human cervical spine and the Hybrid III neckform in combined axial and bending deformations. In all test modes (axial compression, tension-extension, tension-flexion, tension-lateral bending, compression-extension, compression-flexion, compression-lateral bending) there was a large difference between the responses of spines in the fully equilibrated and mechanically stabilized states. In all test modes, the time-dependent responses included a significant viscoelastic exponential relaxation. The hysteresis and stiffness of the human specimens was only weakly dependent on strain rate.

There was a significant difference between the stiffness of the cadaver cervical spines and the Hybrid III. This was expected, since the performance requirements of the Hybrid III were based on human volunteer data, and it is considered to represent a tensed human neck while the cadaver spines have no musculature present (19). The Hybrid III responses were the typical linear viscoelastic type. That is, a linear differential equation would provide an adequate model. The behavior of the human cervical spine was more complex, however, and requires a quasi-linear model (6).

The bending stiffness of the cervical spine was significantly influenced by the direction of the bending moment, the types of end restraint, the magnitude of the deformation, and the previous deformation history. After approximately thirty deformation cycles a mechanically stabilized state was attained that provided repeatable load-deformation responses. The tensile modes were consistently stiffer than the compressive modes. This may be due to a shift in the neutral axis toward the tensile side which pre-tensions slack ligaments and reduces the eccentricity.

Simple beam theory predicts doubling of the bending stiffness when comparing pinned-pinned and fixed-pinned ends. These tests showed an increase in stiffness of approximately eight times. The test apparatus used in these tests (and by most other researchers) constrained the pinned end to move in a straight line. This produced a shearing force which, acting over a relatively long moment arm, stiffened the specimen. This shearing force not only changes the moment acting on the specimen but also influences the failure mode. Several researchers have tested cervical specimens without well controlled and monitored end conditions. Most other works report only the axial load. These experiments indicate that when the loading is eccentric (as it almost always is), the primary deformation mode is bending; and the moment applied to the specimen is strongly influenced by shear forces and the magnitude of the eccentricity. The axial load is therefore a poor indicator of the type and magnitude of failure stresses.

After failure loading many of the specimens imaged with plain radiographs, computed tomography and 1.5 Tesla MRI to detect patterns of injury and to determine the efficacy of each imaging modality in detecting spinal injury.

Complete tears, buckling and stripping, as well as more subtle disruptions of the ligamentum flavum, capsular, anterior and posterior longitudinal ligaments were observed on MR examination. Over 90% of the ligamentous injuries were accurately depicted by MR. MR was clearly superior to CT in detecting soft tissue and ligamentous injuries. Studies in patients suggest that MR demonstration of these injuries *in vivo* is also feasible.

ACKNOWLEDGEMENTS

This work was supported by the Department of Health and Human Services, Center for Disease Control grant R49/CCR402396-02.

BIBLIOGRAPHY

1. Sances, A, Weber, R.C., Larson, S.J., Cusick, J.S., Myklebust, J.B., and Wash, P.R., "Bioengineering Analysis of Head and Spine Injuries," *CRC Critical Reviews in Bioengineering*, February, 1981.

2. Messerer, O., *Uber Elasticitat and Festigkeit der Meuschlichen Knochen*, J. G. Cottaschen Buchhandling, Stuttgart, 1880.

3. Bauze, R.J. and Ardran, M.J., "Experimental Production of Forward Dislocation in the Human Cervical Spine". *Journal of Bone and Joint Surgery*, 60B(2):239, 1978.

4. Sances Jr., A., Myklebust, J., Houterman, C., Webber, R., Lepkowski, J., Cusick, J., Larson, S., Ewing, C., Thomas, D., Weiss, M., Berger, M., Jessop, M.E., Saltzberg, B., "Head and Spine Injuries." *AGARD Conference Proceedings on Impact Injury Caused by Linear Acceleration — Mechanism, Prevention, and Cost*, 1982.

5. McElhaney, J.H., Roberts, V.L., Paver, J.G. and Maxwell, G.M., "Etiology of Trauma to the Cervical Spine," in *Impact Injury to the Head and Spine*, C.C. Thomas, 1982.

6. McElhaney, J.H., Paver, J.G., McCrackin, H.J., and Maxwell, G.M., "Cervical Spine Compression Responses," SAE Paper No. 831615, 1983.

7. Panjabi, M.M., White, A.A., and Johnson, R.M., "Cervical Spine Mechanics as a Function of Transection of Components," *Journal of Biomechanics*, 8(5):327, 1975.

8. Selecki, B.R., and Williams, H.B.L., "Injuries to the Cervical Spine and Cord in Man," Australian Med. Assoc., Mervyn Archdall Med. Monograph #7, Australian Medical Publishers, South Wales, 1970.

9. Nusholtz, G.S., Melvin, J.W., Huelke, D.F., Alem, N.M., and Blank, J.G., "Response of the Cervical Spine to Superior-Inferior Head Impact," *Proc. of the 25th Stapp Car Crash Conference*, SAE Paper No. 811005, pp. 197-237, 1981.

10. Edwards, W.T., Hayes, W.C., Posner, I., White, A.A. III, and Mann, R.W., "Variation of Lumbar Spine Stiffness With Load," *Journal of Biomechanical Engineering*, 109:35, 1987.

11. Markolf, K.L., and Steidel, R.S., Jr., "The Dynamic Characteristics of the Human Intervertebral Joint," ASME Paper No. 70-WA/BHF-6, 1970.

12. Panjabi, M.M., Brand, R.A., Jr., and White, A.A., "Three Dimensional Flexibility and Stiffness Properties of the Human Thoracic Spine," *Journal of Biomechanics*, 9:185, 1976.

13. Roaf, R., "A Study of the Mechanics of Spinal Injury," *Journal of Bone and Joint Surgery*, 42B:810, 1960.

14. Tencer, A.F., Ahmed, A.M., and Burke, D.L., "The Role of Secondary Variables in the Measurement of the Mechanical Properties of the Lumbar Intervertebral Joint," *Journal of Biomechanical Engineering*, 103:129, 1981.

15. Hodgson, V.R., and Thomas, L.M., "The Biomechanics of Neck Injury From Direct Impact to the Head and Neck," Head and Neck Injury Criteria, U.S. Government Printing Office, 1981.

16. Seemann, M.R., Muzzy, W.H. and Lustick, L.S., "Comparison of Human and Hybrid III Head and Neck Response," *Proc. of the Thirtieth Stapp Car Crash Conference*, 1986.

17. Hirsch, C., "Method of Stabilizing Autopsy Specimens in Biomechanical Experiments," *Acta Orthopaedica Scandinavia*, 34(4):374, 1964.

18. Fung, Y.C., "Stress-Strain History Relations of Soft Tissue in Simple Elongations," *Biomechanics — Its Foundation and Objectives*, Prentice-Hall, Inc., Englewood Cliffs, 1972.

19. Mertz, H.J., Neathery, R.F., and Culver, C.C., "Performance Requirements and Characteristics of Mechanical Necks, in *Human Impact Response*, Plenum Press, 1973.